International Journal of Power Electronics and Drive System (IJPEDS)
Vol. 7, No. 4, December 2016, pp. 1240~1251
ISSN: 2088-8694, DOI: 10.11591/ijpeds.v7i4.pp1240-1251

Comparison of Sine and Space Vector Modulated Embedded Z-source Inverter fed Three Phase Induction Motor Drive System

R. Malathi, M. Rathinakumar
Department of Electrical and Electronic Engineering, SCSVMV University, Enathur, Kanchipuram, India

Article Info

Article history:

Received Apr 8, 2016
Revised Nov 13, 2016
Accepted Nov 25, 2016

Keyword:

Embedded Z source inverter (EZSI)
Shoot-through
Sine PWM
Space vector modulation (SVM)
Z source inverter (ZSI)

ABSTRACT

This paper deals with performance of photovoltaic powered Embedded Z-Source Inverter (EZSI) fed Induction motor drive. The DC output from the PV-Panel is boosted and converted into AC using Embedded Z-Source Inverter. EZSI system based on the concept of Z-Source Inverter (ZSI), which provides single stage power conversion. The EZSI also produce same voltage gain as that of the ZSI based system. In EZSI the DC source is embedded within the X-shaped LC impedance network, due to this EZSI has the added advantage of inherent source filtering capability, this can be achieved without any extra passive filter. EZSI can produce the AC output voltage which is greater than the DC link voltage. EZSI system also provides ride-through capability under voltage sags. In this paper the performance of space vector modulated EZSI fed Induction Motor Drive is compared with sinusoidal PWM controlled EZSI fed Drive system. The PV powered EZSI fed three phase Induction Motor System is designed, modeled and simulated using MAT LAB-SIMULINK and the corresponding results are presented. This drive system has advantages like voltage boosting ability and reduced harmonic content.

Corresponding Author:

R. Malathi,
Department of Electrical and Electronic Engineering,
SCSVMV University, Enathur,
Kanchipuram, -631561, India.
E-mail: malathinandhini@yahoo.co.in

1. INTRODUCTION

The applications of renewable energy sources are increasing widely. Among the various renewable energy sources, solar energy finds many applications in standalone systems and distributed generation systems [1]-[2]. Since the solar cell generates a low output voltage, PV system employs single stage power conversion or two stage power conversion based on the requirement to improve its output voltage [3]-[5]. The traditional two stage power converters such as voltage- source inverter (VSI) and current-source inverter (CSI) are either a boost or a buck converter and not a buck-boost converter. When any two switches of the same phase leg are turned ON shoot through would occur and destroy the devices which is a major killer of the converter reliability. The main circuit of VSI and CSI cannot be interchanged. The above mentioned problems are overcome by the Z-source inverter with a single stage power converter proposed in [6]. The Z-source inverter employs a unique LC impedance network to connect the converter main circuit to the power source. Shoot-through zero state is possible with impedance network. The inverter bridge is equivalent to a short circuit when it is in the shoot-through zero state. Without change the total zero- state time interval, shoot-through zero states are evenly allocated into each phase, the active states are unchanged. Because of this shoot- through zero state the DC link voltage of the inverter is boosted. As the voltage generated by the PV panel purely depends on climatic conditions, this Z-source inverter provides a feasible single stage power

conversion. Various modulation strategies have been developed and applied to the Z-Source Inverter to improve the voltage gain and reduce the harmonics [7]-[10]. Different topological developments of Z-Source Inverter for various applications are discussed in [11]-[17]. Modeling, analysis and controlling of Z-Source Inverter has been discussed in [18]-[20]. But the impedance network draws chopping current from the source. This chopping current raises the semiconductor current rating and also complicates the maximum power point tracking(MPPT).Second order LC filter can be placed before the diode D, to reduce high frequency current ripple, but this increases the overall cost as well as resulting in dynamic and resonant problems. To maintain smooth voltage/current across the DC source without adding the external LC filter, the new topology of Z-source network named as Embedded Z-Source Inverter (EZSI) was proposed and analyzed in [21]-[23]. The above literature does not deal with the comparison of sinusoidal PWM controlled EZSI fed induction motor and space vector modulated EZSI fed induction motor.

2. OPERATING PRINCIPLE OF EMBEDDED EZ-SOURCE INVERTER

The two level voltage type EZ-source is shown in Figure 1 has its two dc sources each of $V_{dc}/2$ are embedded within the X shaped LC impedance network. The impedance network is a symmetrical network it is assumed that the value of inductances L_1=L_2=L and the value of capacitances C_1=C_2=C. The inductive elements present in the network are used for filtering the current drawn from the two DC sources; this eliminates the requirement of external LC filter and the size of the capacitor is also reduced [21]. As the impedance network is added with the three phase inverter bridge circuit any two switches can be turned on safely inorder to introduce the shoot-through or short circuit state.Since the current paths in DC frontend are effectively limited by inductive element L_1, L_2 or by both.The inserted shoot-through exhibit the voltage boosting capability, just like Z-Source inverter and can be proven with the gain expression derived from the inverter-state equations during shoot-through and non-shoot-through states expressed by (1)-(4). The non-shoot throuh state can represent any of its six traditional active states (i_1≠0) along with two null states (i_1=0) are solely determined by the modulation process.

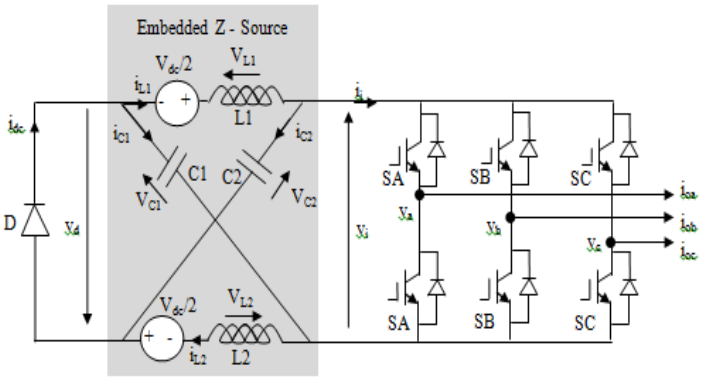

Figure 1. Two level voltage type Three-phase Embedded Z-Source Inverter

EZSI has shoot-through zero state as in ZSI. The equivalent circuit of EZSI during shoot-through state is shown in Figure 2 (a). The front-end diode D is reverse biased when the circuit is in its shoot-through state. The equivalent circuit of EZSI for non shoot through state is shown in Figure 2 (b).

2.1. Active state

The inverter is operated in one of its six active states. The diode D is forward biased. The load and the Inverter bridge is replaced by the current source as shown in Figure 2(b). (The switches Sx ≠ Sx', x = A, B, or C; D = ON. For time interval T_1)

$$V_L = {}^{V_{dc}}/_{2} - V_C \qquad V_i = V_C - V_L + \frac{V_{dc}}{2} = 2V_C \qquad V_d = V_D = 0 \qquad (1)$$

$$i_{dc} = i_L + i_C \qquad i_i = i_L - i_C \qquad i_{dc} \neq 0 \qquad (2)$$

2.2. Nonshoot-Through zero state

Inverter bridge is operating in any one of its two nonshoot-through zero states. Inverter short circuits the load through either upper or lower three switches. The bridge can be viewed as a open circuit. The input DC voltage appears across the inductor and capacitor. But no inverter output current flows to the load. During nonshoot-through zero state the switches Sx ≠ Sx', x = A, B, or C; D = ON.

$$V_L = {}^{V_{dc}}/_{2} - V_C \qquad V_i = 2V_C \qquad V_d = V_D = 0 \tag{3}$$

$$i_{dc} = i_L + i_C \qquad i_i = 0 \qquad i_{dc} \neq 0 \tag{4}$$

2.3. Shoot-through zero state

Shoot through zero state is possible by seven different ways. Without disturbing the active states, shoot-through state is allocated into each phase within total zero time. The front-end diode D is reverse biased. The inverter is viewed as a short circuit from its DC link. There is no voltage across the load but the capacitor voltage is boosted based on the shoot through duty ratio. (The switches Sx = Sx' = ON, x = A, B, or C; D = OFF. For time interval (T_0)

$$V_L = V_C + {}^{V_{dc}}/_{2} \qquad V_i = 0 \qquad V_d = V_D = -2V_C \tag{5}$$

$$i_L = -i_C \qquad i_i = i_L - i_C \qquad i_C = 0 \tag{6}$$

Averaging of voltage across the inductor over a switching period results in the following set of equations for V_C is the capacitive voltage, V_i is the DC- link voltage, V_d =V_D= voltage across the front-end diode, $\hat{V}_i$ *is* the peak DC- link voltage, $\widehat{V_{AC}}$ peak ac output voltage are obtained.

$$V_C = \frac{{}^{V_{dc}}/_{2}}{1-\ 2\,T_0/T} \tag{7}$$

$$\hat{V}_i = \frac{{}^{V_{dc}}/_{2}}{1-\ 2\,T_0/T} = BV_{dc} \tag{8}$$

$$\widehat{V_{ac}} = M\frac{\hat{V}_i}{2} = \frac{MV_{dc}}{2(1-\ 2\,T_0/T)} = B\left(\frac{MV_{dc}}{2}\right) \tag{9}$$

In the above equations T_0/T refers the shoot-through duty ratio (T_0/T < 0.5) per switching period. M represents the modulation index and B is the boost factor, B=1/(1−2 T_0/T). The boost factor B in the above expression is due to the existence of shoot-through states in the switching sequence of the three phase inverter switches.

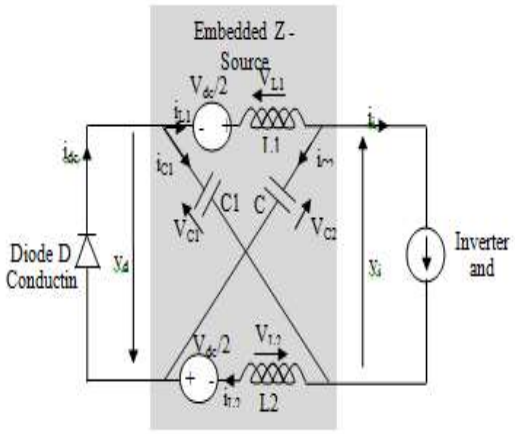

Figure 2(a). Equivalent circuit of two-level EZ-source inverter when in shoot-through state

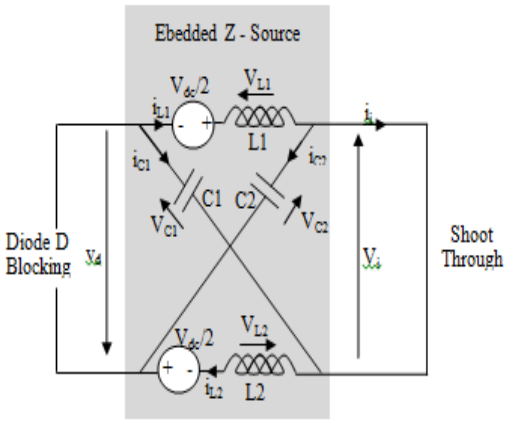

Figure 2(b). Equivalent circuit of two-level EZ-source inverter when in nonshoot-through state

3. SINUSOIDAL PULSE WIDTH MODULATION

Many modulation techniques have been developed and applied to ZSI and the same can be applied to EZSI also. In traditional sine PWM, three phase sinusoidal reference signal with 120 degree phase shift is compared with the triangular carrier signal to generate the gating signals. When the magnitude of the reference signal is greater than the carrier signal, the upper power switch in the respective phase is ON, the reference signal is lesser than the carrier signal, and the power switch is OFF. The complement signals are given to the lower switch of the same phase [9]. This is the maximum boost control method of sine PWM controlled EZSI. In this method all the traditional non-shoot through zero states turned into shoot-through zero states with six active states remains unchanged. The switching sequence for VSI is derived first, then the shoot through states are allocated within the non-shoot through zero states without disturbing the active states. Figure 3, shows the switching pulses along with shoot-through zero states. As all the non-shoot through zero states are turned into shoot-through zero states maximum shoot-through time T_0 and boost factor B are obtained for any given modulation index M. The maximum boost control method introduces a low frequency current ripple in inductor current and capacitor voltage [8]. In this method shoot-through zero state repeats periodically in every n/3 degrees , with the assumptions that switching frequency is much higher than the modulation frequency, the average duty ratio over one switching cycle can be expressed in [8] as follows,

$$D_0 = \frac{2\pi - 3\sqrt{3}\pi}{2\pi} \tag{10}$$

The Boost factor is given by

$$\mathrm{B} = \frac{1}{1 - 2\mathrm{D}_0} = \frac{1}{1 - 2\frac{\mathrm{T}_0}{\mathrm{T}}} \tag{11}$$

The relationship of modulation index and gain,

$$\mathrm{M} = \frac{\pi \mathrm{G}}{3\sqrt{3}\mathrm{G} - \pi} \tag{12}$$

Then,

$$\mathrm{B} = \frac{3\sqrt{3}\mathrm{G} - \pi}{\pi} \tag{13}$$

The voltage stress on the switch is,

$$\mathrm{V_S} = \mathrm{B} * \mathrm{V_{dc}} = \frac{3\sqrt{3}\mathrm{G} - \pi}{\pi}\,\mathrm{V_{dc}} = \frac{\pi}{3\sqrt{3}\mathrm{G} - \pi}\mathrm{V_{dc}} \tag{14}$$

4. SPACE VECTOR MODULATION (SVM)

SVPWM is an advance computation intensive PWM method most suitable modulation technique for variable-frequency drive system. SVPWM technique provides higher inverter output voltage to the motor with lower harmonic distortion. SVPWM is a different approach from PWM modulation based on space vector representation of the voltage in the α-β plane. Space vector concept derived from the rotating magnetic field of the induction motor is used to modulate the inverter output voltage. In SVPWM technique the three phase quantities can be transformed into their equivalent two-phase quantity either in synchronously rotating frames or stationary frame. The voltage vector is used as the reference vector; this gives the advantage of a better overview of the system [10]. In this proposed SVPWM technique, switching sequence for VSI using SVPWM have been generated and then shoot through states can be allocated within the non-shoot through zero states without altering the active state of the switching sequence.

The three phase PWM VSI is shown in Figure 4, In traditional VSI the switching variables a, a', b, b', c and c' controls the switching of the power switches S_1 to S_6. When the upper switch is ON i.e a, b or c is 1, the corresponding lower switch is switched OFF i.e a', b', c' is zero. Therefore ON and OFF states of the upper switches S_1, S_3 and S_5 determines the output voltage. The eight possible switching states are represented as vectors in SVPWM, (V_1 to V_6) are active vectors, V_0 and V_7 are two zero vectors applying zero voltage across the load. The eight possible switching states for the PWM VSI, with six active states and two zero states are given in Table 1.

The relationship between the switching variable vector $[a,b,c]^t$,line-to-line output voltage $[V_{ab}\ V_{bc}\ V_{ca}]^t$ and the phase voltage vector $[V_a\ V_b\ V_c]^t$ are expressed.

$$\begin{bmatrix} v_{ab} \\ v_{bc} \\ v_{ca} \end{bmatrix} = V_{dc} \begin{bmatrix} 1 & -1 & 0 \\ 0 & 1 & -1 \\ -1 & 0 & 1 \end{bmatrix} \begin{bmatrix} a \\ b \\ c \end{bmatrix} \quad (15)$$

$$\begin{bmatrix} v_a \\ v_b \\ v_c \end{bmatrix} = 1/3\ V_{dc} \begin{bmatrix} 2 & -1 & -1 \\ -1 & 2 & -1 \\ -1 & -1 & 2 \end{bmatrix} \begin{bmatrix} a \\ b \\ c \end{bmatrix} \quad (16)$$

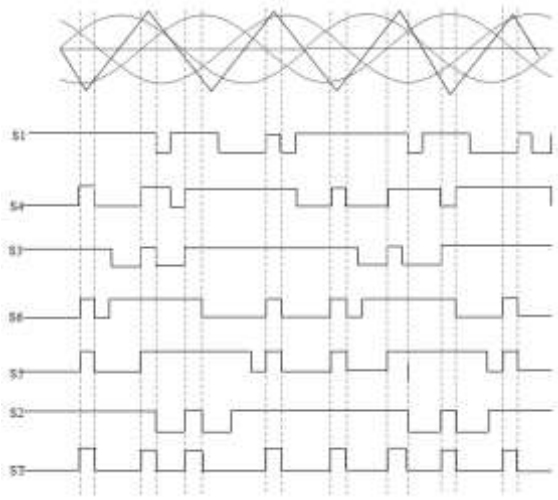

Figure 3. Sin PWM with shoot-through states

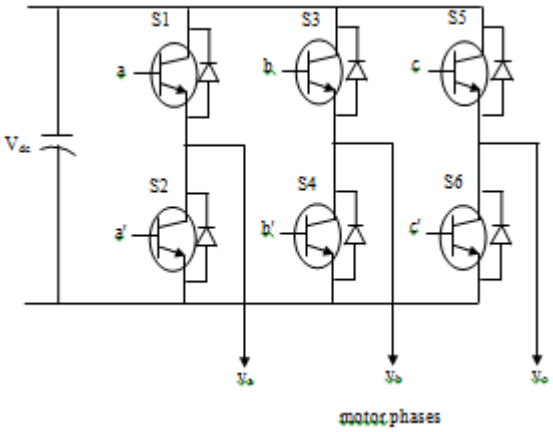

Figure 4. Three phase Voltage Source Inverter

Table 1. Switching vectors, phase voltages and output line to line voltage

Voltage Vectors	Switching vectors			Line to Neutral Voltage			Line to Line Voltage		
	A	b	c	V_a	V_b	V_c	V_{ab}	V_{bc}	V_{ca}
V_0	0	0	0	0	0	0	0	0	0
V_1	1	0	0	2/3	-1/3	-1/3	1	0	-1
V_2	1	1	0	1/3	1/3	-2/3	0	1	-1
V_3	0	1	0	-1/3	2/3	-1/3	-1	1	0
V_4	0	1	1	-2/3	1/3	1/3	-1	0	1
V_5	0	0	1	-1/3	-1/3	2/3	0	-1	1
V_6	1	0	1	1/3	-2/3	1/3	1	-1	0
V_7	1	1	1	0	0	0	0	0	0

4.1. Device On/Off States and Corresponding Outputs of a Three Phase VSI

The vector representation of the phase voltages corresponding to the eight combinations can be obtained by applying α-β transformation to the phase voltage. This transformation is equivalent to an orthogonal projection of $[a\ b\ c]^t$ onto the two dimensional plane perpendicular to the vector $[1\ 1\ 1]^t$ in a three dimensional co-ordinate system which results in six non-zero vectors (V_1-V_7) and two zero vectors (V_0 and V_7). The non-zero vectors forms the axes of a hexagonal. The angle between any two adjacent non-zero vector is 60 degrees. The zero vectors are at the origin and apply zero voltage to a three phase load. The eight vectors are called basic space vectors and are shown in Figure 5. The reference voltage vector in αβ-plane is shown in Figure 6. This is a two-dimensional plane transformed into a three-dimensional plane, containing vectors of three phase voltages.

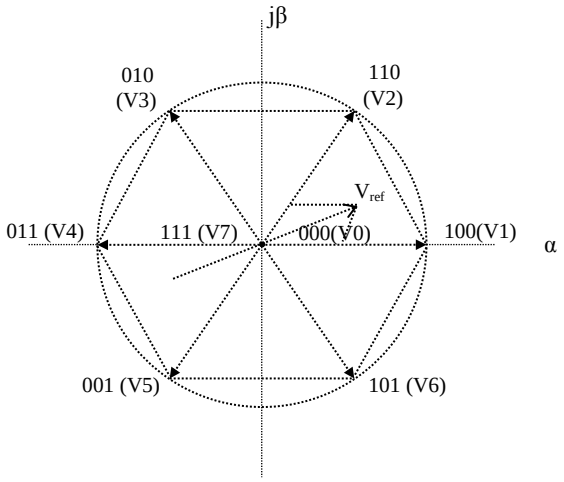

Figure 5. Space Voltage Vectors in Different Sectors

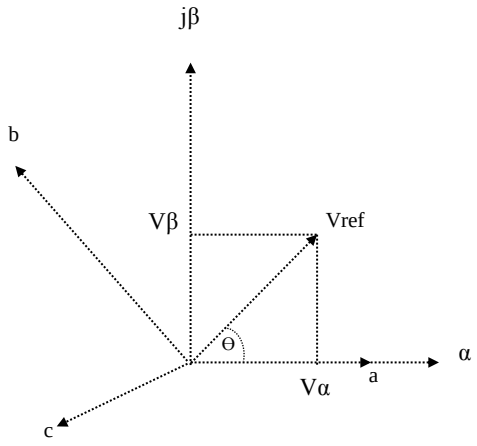

Figure 6. Reference Vector in the Two and Three Dimensional Plane

The ON and OFF state of the switches are determined by the location of the reference vector on the αβ-plane. The relationship between these two frames is given,

$$f_{\alpha\beta 0} = k_s f_{abc} \tag{17}$$

where k_s is,

$$K_S = \frac{2}{3}\begin{bmatrix} 1 & -1/2 & -1/2 \\ 0 & \sqrt{3/2} & \sqrt{3/2} \\ 1/2 & 1/2 & 1/2 \end{bmatrix} \tag{18}$$

Here *f* denotes either a voltage variable or a current variable. The objective of the SVPWM technique is to approximate the reference voltage Vref instantaneously by combination of the switching states corresponding to the basic space vectors. The magnitude and angle of the reference voltage vector can be calculated using clerk's transformation.

$$V_{ref} = V_\alpha + jV_\beta = \frac{2}{3}(V_a + aV_b + a^2V_c) \tag{19}$$

Where 'a' is given by $a = e^{j2\pi/3}$

The magnitude of $|V_{ref}| = \sqrt{V_\alpha^2 + V_\beta^2}$

Angle $\theta = \tan^{-1}\left(V_\beta / V_\alpha\right)$

$$V_\alpha = \frac{2}{3}\left(V_a - \frac{1}{2}V_b - \frac{1}{2}V_c\right) \tag{20}$$

$$V_\beta = \frac{2}{3}\left(\frac{\sqrt{3}}{2}V_b - \frac{\sqrt{3}}{2}V_c\right) \tag{21}$$

The next step is to calculate the duration time for each vector V_1–V_6. The switching time duration at any sector can be obtained as follows,

$$T_1 = \frac{\sqrt{3}}{V_{dc}} \frac{T_s.\overline{V}_{ref}}{} (sin\frac{n}{3}\pi.cos\theta - cos\frac{n}{3}\pi.sin\theta) \quad (22)$$

$$T_2 = \frac{\sqrt{3}}{V_{dc}} \frac{T_s.\overline{V}_{ref}}{} (cos\theta.sin\frac{n-1}{3}\pi + sin\theta.cos\frac{n-1}{3}\pi) \quad (23)$$

$$T_0 = T_s - T_1 - T_2 (0 \leq 0 \leq 60^0) \quad (24)$$

Where, n=1 through 6 (i.e., sector 1 to 6) and $D_0 = T_0 / T_s$ Shoot through duty ratio

$$D_0 = \frac{3}{4} * \frac{2\pi - 3\sqrt{3}M}{2\pi}$$

Boost factor (B), can be found as,

$$B = \frac{4\pi}{9\sqrt{3}M - 2\pi} \quad (25)$$

Similarly, the voltage gain can be found as;

$$G = \frac{\widehat{V_1}}{V_{dc}/2} = \frac{4\pi M}{9\sqrt{3}M - 2\pi} \quad (26)$$

The voltage stress across the devices can be;

$$V_S = \frac{9\sqrt{3}G - 4\pi}{2\pi} V_{dc} \quad (27)$$

The switching pattern is obtained with SVM technique then shoot-through states (ST) are allocated into each phase. This is shown in Figure 7.

5. SIMULATION RESULTS

The simulation circuit of sine PWM controlled two level voltage type Embedded Z-Source Inverter fed three phase Induction Motor drive is shown in Figure 8, two similar PV-source each of delivering $V_{dc}/2$= 24 volts are used as a DC source of EZ-network. Simulation circuit for EZSI fed three phase induction motor is modeled and simulated using MATLAB/SIMULINK. The simulation is carried out with $L_1=L_2$=20mH, $C_1=C_2$=2200μf. The solar output voltage of $V_{dc}/2$=24 volts is applied to EZS network. The boosted output voltage of Embedded Z-Source network with the duty ratio T_0/T = 0.25 is 96 volts shown in Figure 9. The shoot-through states are allocated in the switching sequence and the switching pulses generated for the switches. The three phase output voltages are shown in Figure 10. The speed of the motor increase with an increase in voltage and settles at 1000 RPM, is shown in Figure 11. The FFT analysis of the inverter output voltage is done with MATLAB and the Total Harmonic Distortion (THD) 6.01% is measured. The Harmonic Spectra is shown in Figure 12. From the above analysis, the boost factor is given by,

$$B = \frac{1}{1-2\frac{T_0}{T}} = 2 ,$$

The DC link voltage is given by,

The DC $\widehat{V_i} = \frac{V_{dc}/_2}{1-\ 2\ T_0/T} = BV_{dc} = 2 \times 48 = 96\ volts.$

The output peak phase voltage from the inverter can be expressed as

$$\widehat{V_{ac}} = M\frac{\widehat{V_i}}{2} = \frac{MV_{\ dc}}{2(1-\ 2\ T_0/T)} = B\left(\frac{MV_{dc}}{2}\right),$$

With the modulation index M=0.8, $\widehat{V_{ac}} = 40.4\ volts.$

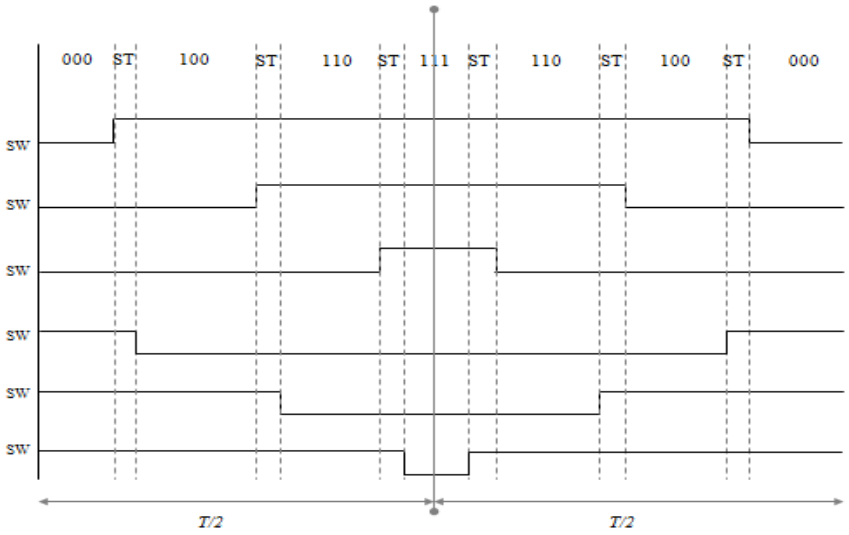

Figure 7. Space Vector modulated switching pulses with shoot-through state

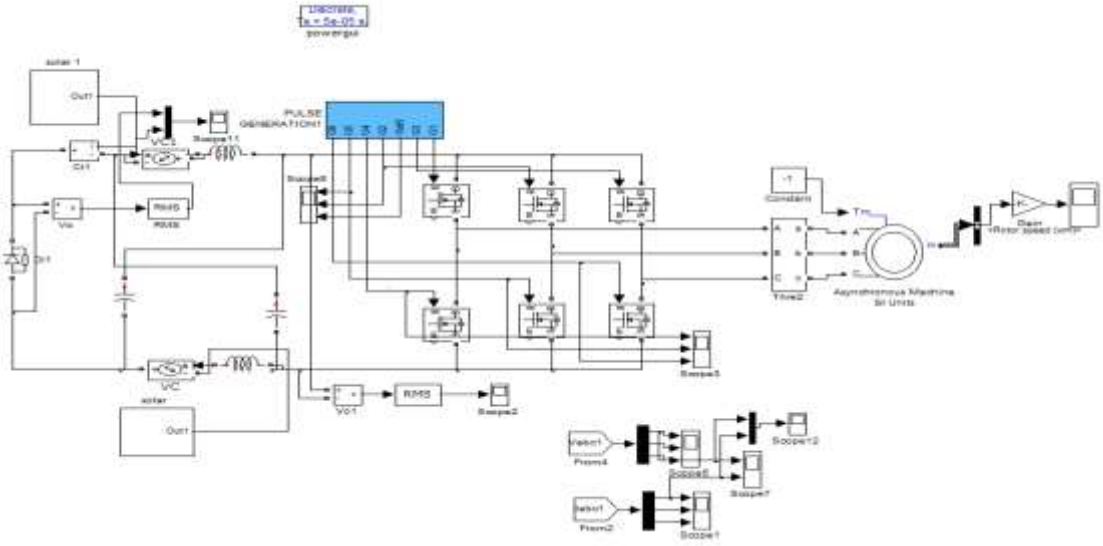

Figure 8. Simulation circuit of Sinusoidal pulse width modulated three phase induction motor drive

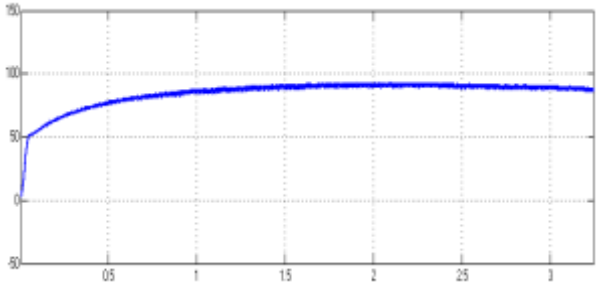

Figure 9. Output voltage of Embedded Z-Source

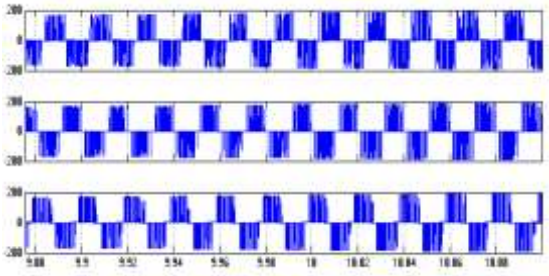

Figure 10.Output phase voltages of three phase EZSI

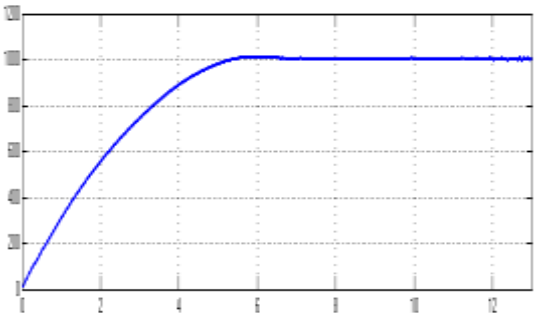

Figure 11. Motor Speed

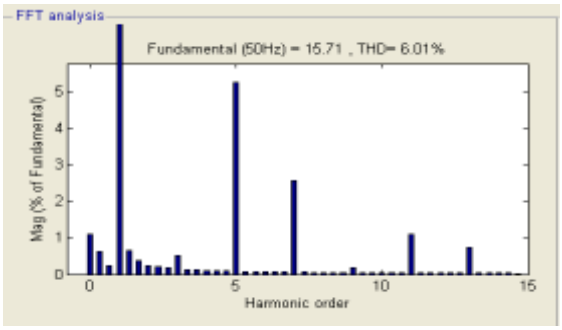

Figure 12. Harmonic Spectrum

5.1. SVM Controlled Induction Motor Drive

The simulation circuit for space vector modulated EZSI fed three phase induction drive is shown in Figure 13. The sine PWM generation block is replaced by SVM block. The solar output voltage of Vdc/2= 24 volts is shown in Figure 14. The boosted output voltage of EZ-NETWORK with the duty ratio T_0/T= 0.3 shown in Figure 15, and its value is 120 volts. The three phase voltages are shown in Figure 16. The speed of the three phase induction motor is shown in Figure 17 the speed gradually increases with an increase in voltage at the time of starting and settles at 1200rpm. FFT analysis is done for the inverter output voltage using MATLAB and the measured THD for space vector modulated voltage is 3.87%, Harmonic spectrum is shown in Figure 18.

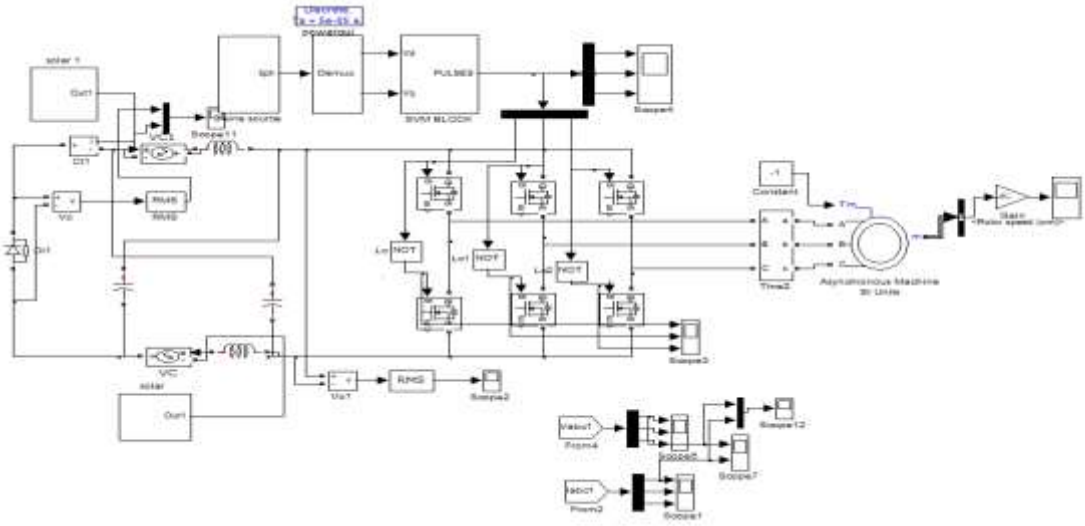

Figure 13. Simulation circuit for SVM EZSI fed three phase induction motor drive

The boost factor is given by,

$$B = \frac{1}{1-2\frac{T_0}{T}} = 2.5 \ ,$$

The DC link voltage is given by

$$\hat{V}_i = \frac{V_{dc}/_2}{1-\ 2\ T_0/T} = BV_{dc} = 2.5 \times 48 = 120\ volts$$

The output peak phase voltage from the inverter can be expressed as

$$\widehat{V_{ac}} = M\frac{\hat{V}_i}{2} = \frac{MV_{dc}}{2(1-2T_0/T)} = B\left(\frac{MV_{dc}}{2}\right),$$

With the modulation index M=0.8, $\widehat{V_{ac}} = 48\ volts$.

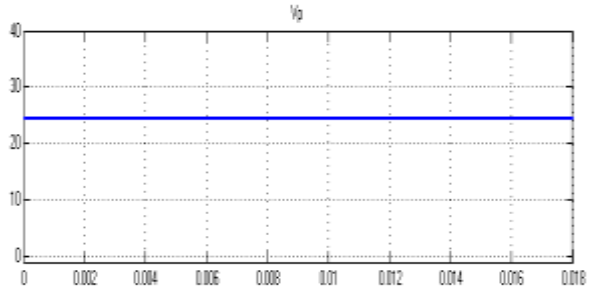

Figure 14. Solar output voltage

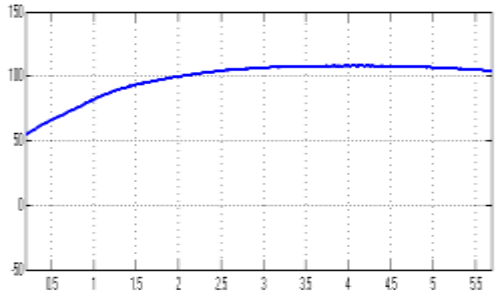

Figure 15. Output voltage of EZS network

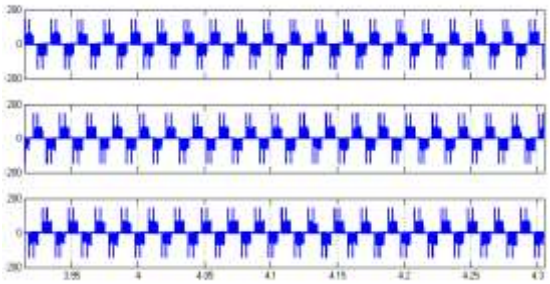

Figure 16. Output phase voltages of three phase EZSI

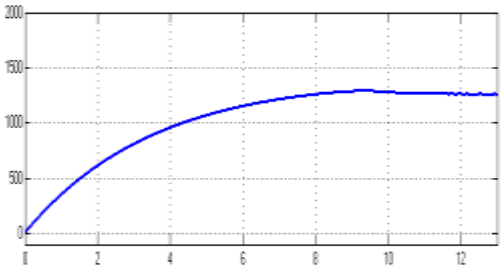

Figure 17. Motor Speed

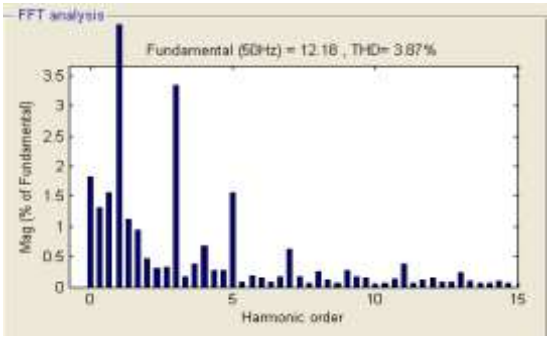

Figure 18. Harmonic Spectrum

Table 2. Comparison of Sine PWM EZSI and SVW EZSI fed induction motor drive

PARAMETERS	Sine PWM	SVM
Input Voltage(V)	24	24
EZ-Output Voltage(V)	96	120
Speed(RPM)	1000	1200
THD%	6.01	3.87

6. CONCLUSION

PV powered Embedded Z-Source Inverter fed three phase Induction motor drive is modeled and simulated successfully with Sine PWM and SVM methods. FFT analysis was done and the details of THD are presented. The simulation results indicate that the harmonic content with SVM is less than that of Sine PWM controlled inverter fed Induction Motor Drive. For the same input voltage of 48 volts SVM provides increased output voltage with increase in speed. The comparison results are presented in Table 2. The drawbacks of this drive system are that it requires two similar PV-sources which increases the initial cost of total drive system.The closed loop controlled induction motor system will be investigated in future.

REFERENCES

[1] Rong-Jong Wai and Wen-Hung Wang, "Grid-connected photovoltaic generation system", *IEEE Trans. circuits and systems*, vol. 55, no. 3, Apr. 2008.

[2] J.A. Gow and C.D. Manning, *"Photovoltaic converter system suitable for use in small scale stand-alone or grid connected applications*", Proc.IEE Electric. Power Appl., vol. 147, no. 6, pp. 535-543, Jun. 2000.

[3] R.O. Caceres and I. Barbi, "A boost DC-AC converter: analysis, design, and experimentation", *IEEE Trans. Power Electronics*, vol. 14, pp. 134-141, 1999.

[4] N. Vazquez, J. Almanan, J. Alvarez, C. Aguilar, and J. Arau, *"Analysis and experimental study of the buck, boost and buck-boost inverters"*, in Proc.IEEE 30th Annu. Power Electron. Spec. Conf., vol. 2, pp. 801-806, 1999.

[5] BbJ. Almazan, N. Vazquez, C. Hemandez, J. Alvarez, and J.Arau, *"A comparison between the buck, boost and buck-boost inverters"*, in Proc. IEEE 7th Int. Power Electron Congr, pp. 341-346, 2000.

[6] F.Z. Peng, Z-Source Inverter, *IEEE Tran. Ind. Tran. Appl*., vol. 39, no. 2, pp. 504-510, Mar/Apr. 2003.

[7] P.C. Loh, D.M. Vilathgamuva, Y.S. Lai, G.T. Chua, and Y.W. Li, "Pulse-width modulation of Z-source inverters", *IEEE Trans. Power Electron, vol. 20*, no 6, pp. 1346-1355, Nov. 2005.

[8] M.S. Shen, J. Wang, A.Joseph, F.Z.Peng, L.M. Tolbert, and D.J. Adams, "Constant boost control of the Z-source inverter to minimize current ripple and voltage stress", *IEEE Trans. Ind. Appl.*, vol. 42, no. 3, pp. 770-777, May/Jun. 2006.

[9] F.Z. Peng, M.S. Shen, and Z. Qian, "Maximum boost control of the Z-source inverter", *IEEE Trans.Power Electron.*, vol. 20, no. 4, pp. 833-838, Jul. 2005.

[10] Yushan Liu, Baoming Ge, Haitham Abu-Rub and Fang Zhang Peng, "Overview of space vector modulations for three-phase Z-source/Quasi-Z-source inverters", *IEEE Trans. Power Electron*., vol. 29, no. 4, Apr. 2014.

[11] P.C. Loh, Feng Gao and Frede Blaabjerg, "Topological and modulation design of three-level inverters", *IEEE Trans. Power Electron*, vol. 23, no. 5, PP. 2268-2277, Sep.2008.

[12] Yu Tang, Shaojan Xie, Chaohua Zhang, Zegang Xu, "Improved Z-Source inverter with reduced Z-source capacitor voltage stress and soft-start capability", *IEEE Trans. Power Electron*., vol. 24, no. 2, pp. 409-415, Feb. 2009.

[13] Zhi Jian Zhou, Xing Zhang, Po Xu and Weixiang X. Shen, "Single-phase uninterruptible power supply based on Z-Source inverter", *IEEE Trans. Ind. Electron*, vol. 55, no. 8, PP. 2297-3004, Aug.2008.

[14] Dong Cao, Shuai Jiang, Xianhao Yu and Fang Zheng Peng, "Low-cost semi-Z-Source inverter for single-phase photovoltaic systems", *IEEE Trans. Power Electron*, vol. 26, no.12, pp. 3514-3523, Dec.2011.

[15] Fang Z. Peng, Xiaoming Yuan, Xupeng Fang, and Zhaoming Qian, " Z-Source inverter for adjustable speed drives", *IEEE Power Electronics Letter*., vol. 1, no.2, pp. 33-35, June.2003.

[16] Dong Sun, Boaming Ge, Fang Zheng Peng, Abu Rub Haitham, Dqiang Bi, Yushan Liu, " A new grid-connected PV system based on cascaded H-bridge Quasi-Z-Source inverter", *IEEE Power Electron. Conf*., pp. 951-956, 2012.

[17] Fang Zheng Peng, Miaosen Shen, Kent Holland, "Application of Z-Source inverter for traction drive of fuell cell-battery Hybrid Electric Vehicles", *IEEE Trans. Power Electron*, vol. 22, no.3, pp. 1054-1061, May. 2007.

[18] Jingbo Liu, Jiangang Hu, and Longya Xu, "Dynamic modeling and analysis of Z-Source converter-Derivation of AC small signal model and design-oriented analysis", *IEEE Trans. Power Electron*, vol. 22, no.5, pp. 1786-1796, Sep. 2007.

[19] Veda Prakash Galigekere and Marian K.Kazimierczuk, *"Small-signal modeling of PWM Z-Source converter by circuit-averaging technique*", IEEE Conf. 2011.

[20] Chadana Jayampathi Gajanayake, D. Mahinda Vilathgamuwa, and Poh Chiang Loh, "Development of a comprehensive model and a multiloop controller for Z-Source inverter DG system", *IEEE Trans. Ind. Electron*, vol. 54, no. 4, PP. 2352-2359, Aug. 2007.

[21] Chiang, Loh, "Embedded EZ-source inverters", *IEEE Trans. Ind. Appl*. vol. 46, no. 1, PP. 256-267, Jan/Feb. 2010.

[22] F. Gao, P.C. Loh, F. Blaabjerg and C.J. Gajanayake, "*Operational analysis and comparative evaluation of Embedded Z-source inverters"*, IEEE conf. 2008.

[23] F. Gao, P.C. Loh, D.Li, and F.Blaabjerg, "Asymmetric and Symmetric Embedded EZ-source inverters", *IET Power Electron*.vol. 4, no. 2, pp. 181-193, 2011.

BIOGRAPHIES OF AUTHORS

Mrs. R. Malathi, born in Cuddalore, Tamilnadu, India, on July 10, 1974. She graduated from Annamalai University under Electrical and Electronics Engineering in the year 1995. She obtained her post graduation in Power Electronics & Industrial Drives from the Sathyabama University in the year 2005. She has put around 18 years of experience in teaching Electrical Engineering. Her areas of interest are Power Electronics, Electric Drives and Renewable energy System. Presently she is working as Associate Professor in the Department of Electrical and Electronics Engineering SCSVMV University, Enathur, Kanchipuram, Tamilnadu, India.

Dr. M. Rathinakumar, born in Madurai, Tamilnadu, India, on July 19, 1969. He graduated from Thiyagarajar College of Engineering, affiliated to Madurai Kamaraj University under Electrical and Electronics Engineering in the year 1993. He obtained his post graduation in Power Systems from the same University in the year 1995.
He obtained his Ph.D from SCSVMV University, Enathur, Kanchipuram, Tamilnadu, India in the year 2010. He has put around 20 years of experience in teaching Electrical Engineering. His areas of interest are Power systems, Power Quality, Power System Operation and Control. Presently he is working as Professor and Head in the Department of Electrical and Electronics Engineering SCSVMV University, Enathur, Kanchipuram, Tamilnadu, India.